

## Supporting Information

### **Probing the Self-discharge Behaviors of LiMn<sub>2</sub>O<sub>4</sub> Cathode at Elevated Temperatures: *In-Situ* X-ray Diffraction Analysis and a Co-Doping Mitigation Strategy**

Xiaoyu Tang,<sup>a</sup> Jie Zhou,<sup>b</sup> Miao Bai,<sup>a</sup> Weiwei Wu,<sup>a</sup> Shaowen Li,<sup>a</sup> and Yue Ma<sup>\*a</sup>

<sup>a</sup> Center for Nano Energy Materials, State Key Laboratory of Solidification Processing School of Materials Science and Engineering, Northwestern Polytechnical University, 710072 Xi'an, China

E-mail: [mayue04@nwpu.edu.cn](mailto:mayue04@nwpu.edu.cn)

<sup>b</sup> Xi'an S.E.E.D energy research center, Xi'an economic & technological development zone, Xi'an, 710018

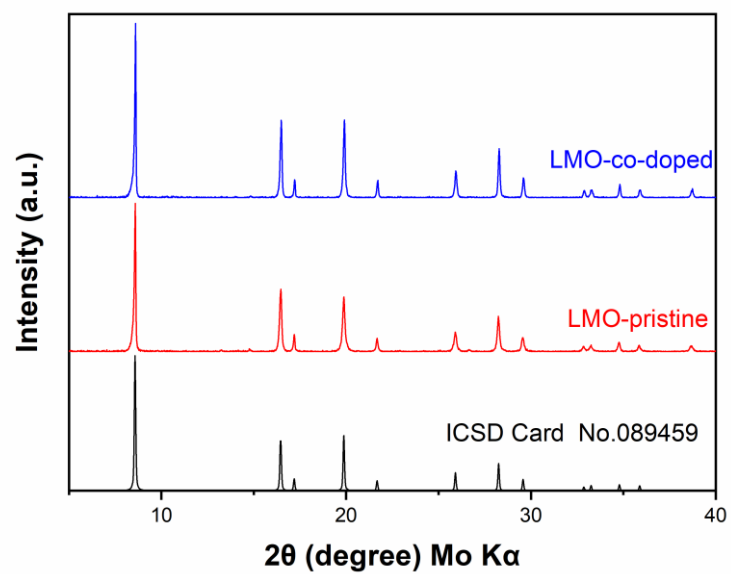
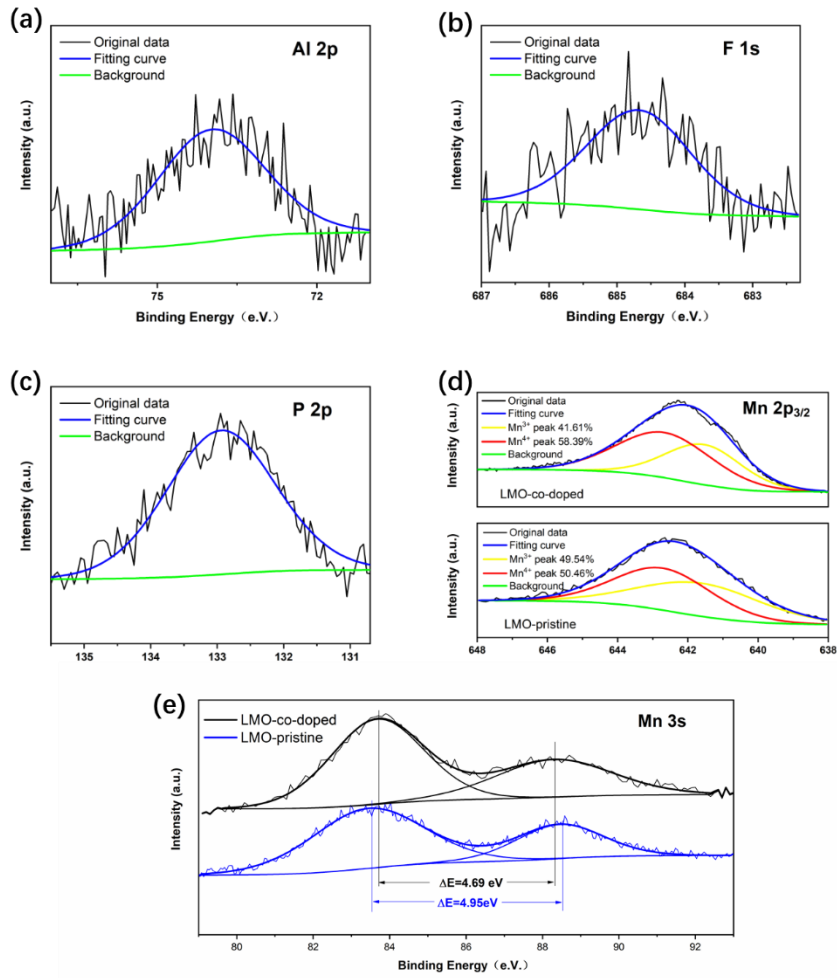
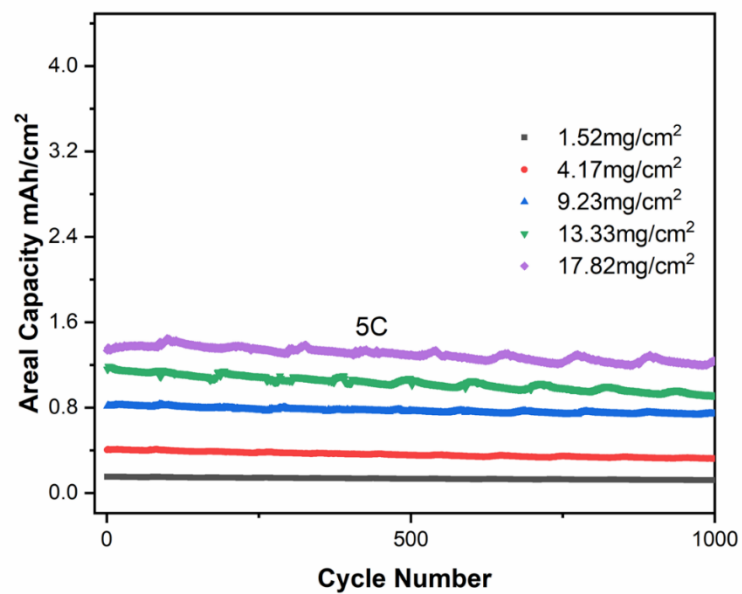


Fig.S1 XRD patterns of LMO-co-doped and LMO-pristine.



**Fig.S2** High resolution XPS spectra of (a) Al 2p, (b) F 1s and (c) P 2p of LMO-co-doped sample. (d) Mn 2p<sub>3/2</sub> of LMO-co-doped and LMO-pristine sample. (e) Mn 3s core-level XPS spectra of LMO-co-doped and LMO-pristine samples.



**Fig.S3** Cycling performance of LMO-co-doped electrode with various loading mass at 5C.

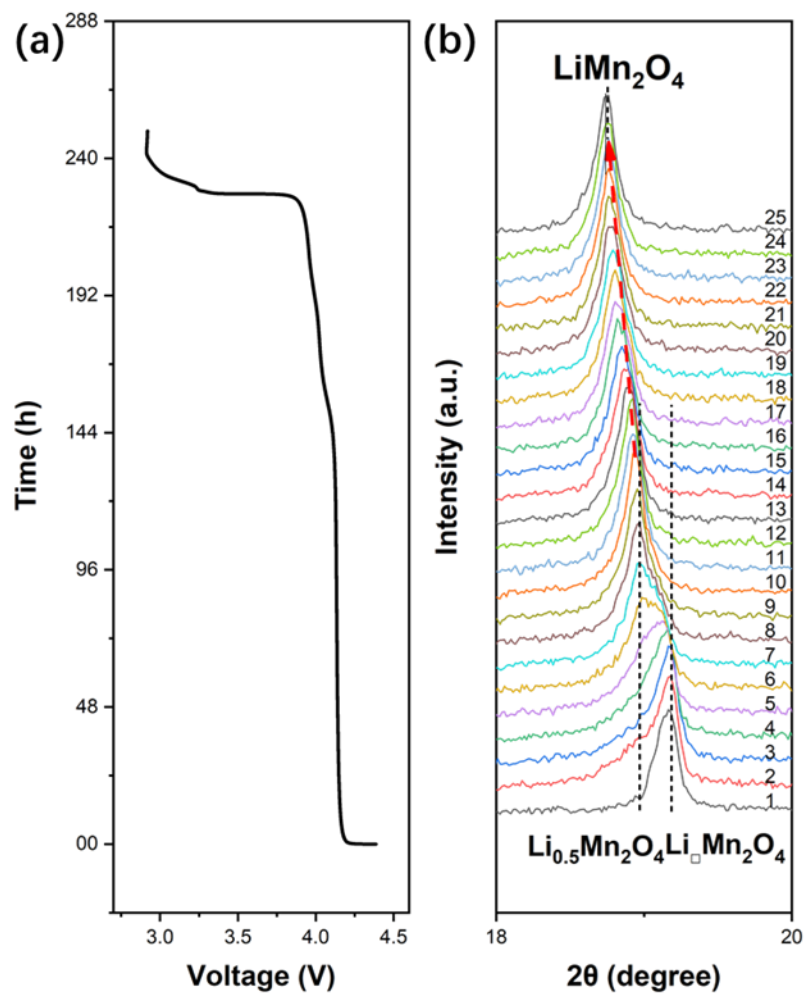


**Fig. S4** (a) The open-circuit voltage profile of the oxidized charged LMO-co-doped at 55 °C. (All test parameters are consistent with Fig. 1) (b) The *in-situ* XRD pattern collected during the self-discharge process. The measured XRD patterns was listed for every 10 hours.

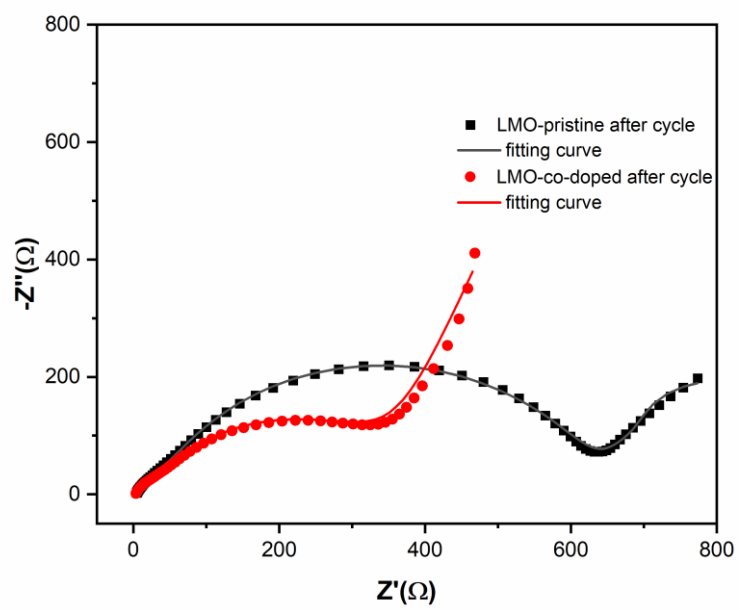


**Fig. S5** EIS spectra of LMO-co-doped and LMO-pristine after 50 cycles at 0.5C.

We further compared the electrochemical performance of the samples with single dopant and co-dopants in Fig. S6. When cycling at 1C at 55 °C, all of the LMO-PO<sub>4</sub><sup>3-</sup> doped, the LMO-Al-doped and the LMO-F-doped cathode samples exhibit an improved capacity retention capability of 89.2%, 83.7% and 81.5% for 100 cycles respectively, as compared to the capacity retention value of 68.4% for pristine LMO sample. While the LMO-co-doped cathode maintain the robust cycling with capacity retention of ~98% for 100 cycles. This comparison result demonstrates the synergistic coupling of Al, F and PO<sub>4</sub><sup>3-</sup> dopants on the structure robustness of the LMO cathode.

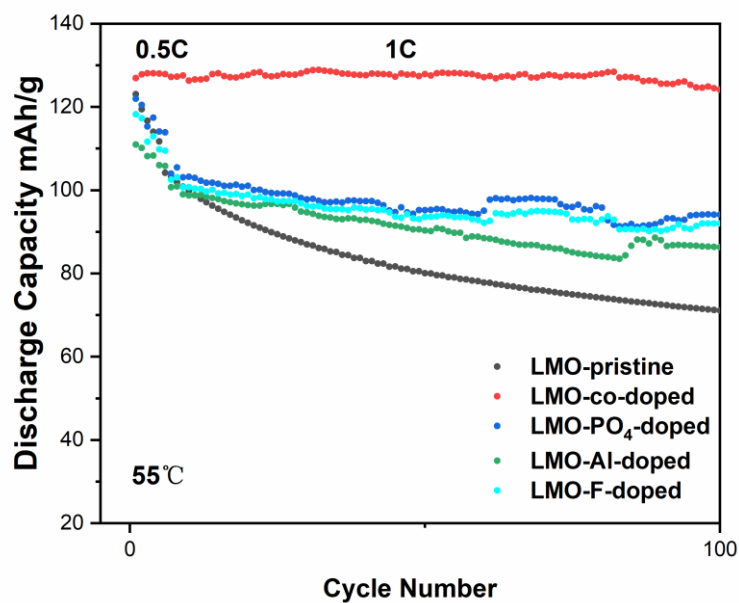


**Fig. S6** Comparison of the cycling performance of LMO-co-doped to the samples with various single dopant at 55 °C.

---

LMO-co-doped after cycle	3.544	26.09	317
LMO-pristine after cycle	4.047	35.63	590.1

---

**Table.S1** Resistances derived from EIS based on the proposed equivalent circuit model.

We compared cycling performance values of the cited reference with our work. As shown in the Table S2, our work demonstrates the cycling performance among the best results as compared to the pioneer studies in terms of specific capacity and capacity retention capability upon cycling. In consideration of the low self-discharge rate at the evaluated temperature and the facile synthesis without complicated morphology control process, our as-developed co-doped LMO cathode could find use in the practical battery applications.

Strategy	Electrochemical performance: initial capacity, capacity retention (cycles, rate, temperature)	Ref
Al doping & Li excess	104.0 mAh g <sup>-1</sup> , 95.8% (100, 1C, 25°C) 105.7 mAh g <sup>-1</sup> , 95.8% (100, 1C, 25°C)	1
Ni doping & Li excess	105.1 mAh g <sup>-1</sup> , 90.4% (100, 1C, 55°C) 105.3 mAh g <sup>-1</sup> , 90.7% (100, 1C, 55°C)	1
Co doping	103 mAh g <sup>-1</sup> , 97.1% (85, 0.1mA/cm <sup>2</sup> , room temperature)	2
Cr doping	122 mAh g <sup>-1</sup> , 94.2% (50, 0.15mA/cm <sup>2</sup> , room temperature)	3
Co doping	123 mAh g <sup>-1</sup> , 92.7% (50, 0.2C, 25°C) 127 mAh g <sup>-1</sup> , 87.4% (50, 0.2C, 55°C)	4
Ni doping	108 mAh g <sup>-1</sup> , 97.2% (100, 0.5C, room temperature)	5
Li & Co doping	100 mAh g <sup>-1</sup> , 86.0% (1000, 2C, room temperature) 100 mAh g <sup>-1</sup> , 85.2% (100, 1C, 55°C)	6
Li <sub>4</sub> Ti <sub>5</sub> O <sub>12</sub> coating	100 mAh g <sup>-1</sup> , 87.1% (45, 0.5C, room temperature) 92 mAh g <sup>-1</sup> , 86.9% (45, 0.5C, 55°C)	7
ZrO <sub>2</sub> coating LMO nanowire	135 mAh g <sup>-1</sup> , 94.8% (55, 1C, 65°C)	8
LiNi <sub>0.05</sub> Mn <sub>1.95</sub> O <sub>4</sub> surface modify	125 mAh g <sup>-1</sup> , 96% (20, 0.5C, room temperature)	9
Li <sub>2</sub> O–2B <sub>2</sub> O <sub>3</sub> (LBO) glass coating	111.3 mAh g <sup>-1</sup> , 100% (30, 1C, room temperature)	10
LiNi <sub>1/2</sub> Mn <sub>1/2</sub> O <sub>2</sub> coating	100 mAh g <sup>-1</sup> , 98% (50, 0.5C, 60°C)	11
Our work	112.20 mAh g <sup>-1</sup> , 95.5% (200, 1C, room temperature) 111.09 mAh g <sup>-1</sup> , 91.8 (1000, 5C, room temperature) 126.92 mAh g <sup>-1</sup> , 97.7% (95, 1C, 55°C)	

**Table. S2** The electrochemical performance comparison between this work and the previously reported work.

The Ragone plots (Fig. S7) compare the present work and the previously reported LMO cathodes from the references. Encouragingly, our LMO-co-doped cathode could output a maximum gravimetric energy density of 455.0 Wh/kg at a power density of 287 W/kg at room temperature. When operating at 55°C, a satisfactory energy density of 497.6 W h kg<sup>-1</sup> and peak power density of 287 W kg<sup>-1</sup> were achieved. As compared to the previously reported LMO cathodes in the references, these energy/power density results are among the best performing electrodes for Li-ion storage.<sup>3-5, 7, 9-11</sup> Some LMO materials,<sup>3, 4, 9</sup> such as LiNi<sub>0.05</sub>Mn<sub>1.95</sub>O<sub>4</sub> modified LMO cathode demonstrates the high energy densities of 512.5 W h kg<sup>-1</sup>; however, the capacity retention is only 96% after 20 cycles. In Fig. S8, we also draw the 3D Ragone plot as a function of cycle number to elaborate the performance comparison easier. For the convenience of observation, we also project the 3D data onto the bottom surface with the same color dots. In consideration of the low self-discharge rate at the evaluated temperature and the facile synthesis without complicated morphology control process, our as-developed co-doped LMO cathode demonstrates great potential for the practical applications. We have incorporated Ragone plot data as Fig. S7 and Fig. S8 in the supporting information as the reviewer suggested.

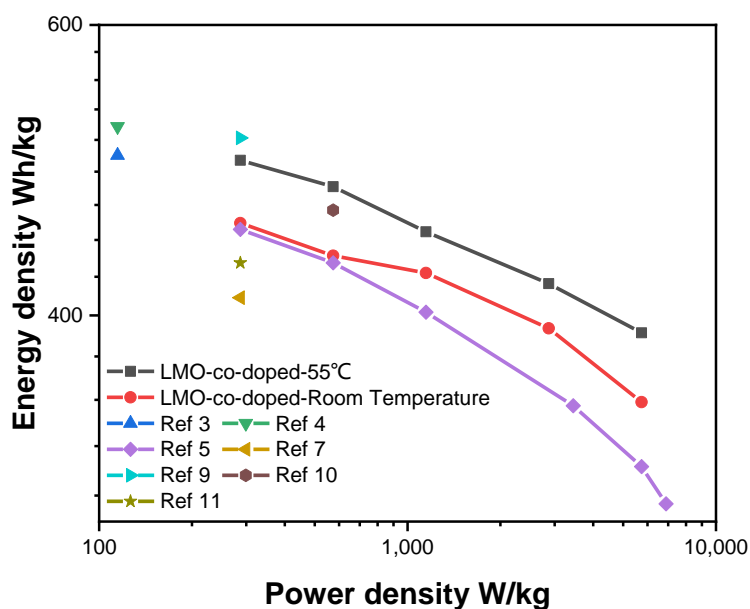


**Fig. S7** Ragone plots of the LMO cathode based on the weight of electrode.

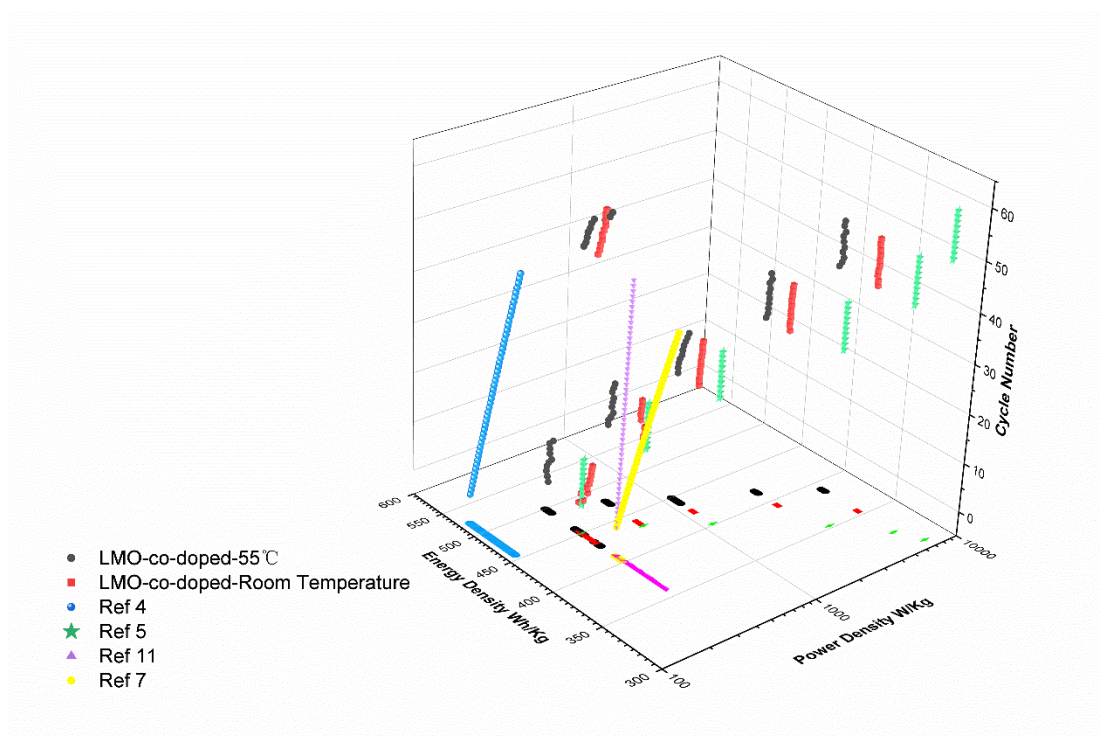


**Fig. S8** 3D Ragone plots of our work and the previously reported LMO cathode.

## Reference

1. J. M. Amarilla, K. Petrov, F. Picó, G. Avdeev, J. M. Rojo and R. M. Rojas, *Journal of Power Sources*, 2009, **191**, 591-600.
2. P. Arora, *Journal of The Electrochemical Society*, 1998, **145**, 807-815.
3. G. X. Wang, D. H. Bradhurst, H. K. Liu and S. X. Dou, *Solid State Ionics*, 1999, **120**, 95-101.
4. H. Huang, C. Wang, W. K. Zhang, Y. P. Gan and L. Kang, *Journal of Power Sources*, 2008, **184**, 583-588.
5. X. Li and Y. Xu, *Applied Surface Science*, 2007, **253**, 8592-8596.
6. C. Wang, S. Lu, S. Kan, J. Pang, W. Jin and X. Zhang, *Journal of Power Sources*, 2009, **189**, 607-610.
7. D.-Q. Liu, X.-Q. Liu and Z.-Z. He, *Materials Chemistry and Physics*, 2007, **105**, 362-366.
8. S. Lim and J. Cho, *Electrochemistry Communications*, 2008, **10**, 1478-1481.
9. Y. F. Yuan, H. M. Wu, S. Y. Guo, J. B. Wu, J. L. Yang, X. L. Wang and J. P. Tu, *Applied Surface Science*, 2008, **255**, 2225-2229.
10. H. Sahan, *Solid State Ionics*, 2008, **178**, 1837-1842.
11. J.-W. Lee, S.-M. Park and H.-J. Kim, *Electrochemistry Communications*, 2009, **11**, 1101-1104.